Article:

Article

Fate of Mixmaster Chaos in a Deformed Algebra Framework

Gabriele Barca [1,*] and Eleonora Giovannetti [2]

[1] School of Mathematical and Physical Sciences, University of Sheffield, Hicks Building, Hounsfield Road, Sheffield S3 7RH, UK

[2] Department of Physics, La Sapienza University of Rome, P.le Aldo Moro, 00185 Roma, Italy; eleonora.giovannetti@uniroma1.it

* Correspondence: gabriele_barca001@ehu.eus

Abstract: We analyze the anisotropic Bianchi models, and in particular the Bianchi Type IX known as the Mixmaster universe, where the Misner anisotropic variables obey Deformed Commutation Relations inspired by Quantum Gravity theories. We consider three different deformations, two of which have been able to remove the initial singularity similarly to Loop Quantum Cosmology when implemented in the single-volume variable. Here, the two-dimensional algebras naturally implement a form of Non-Commutativity between the space variables that affects the dynamics of the anisotropies. In particular, we implement the modifications in their classical limit, where the Deformed Commutators become Deformed Poisson Brackets. We derive the modified Belinskii–Khalatnikov–Lifshitz map in all the three cases, and we study the fate of the chaotic behavior that the model classically presents. Depending on the sign of the deformation, the dynamics will either settle into oscillations between two almost-constant angles, or stop reflecting after a finite number of iterations and reach the singularity as one last simple Kasner solution. In either case, chaos is removed.

1. Introduction

One of the most general predictions of Relativistic Cosmology is the existence of singularities [1,2], where curvature invariants diverge and General Relativity ceases to be predictive. However, it is expected that in the high-energy regimes close to the singularities, quantum effects must come into play.

The two most successful proposals for formulating Quantum Gravity (QG) theories are Loop Quantum Gravity (LQG) [3–5] (see [6,7] for recent reviews) and String Theories (STs) [8–10]. However, their implementation in the cosmological setting, resulting in the frameworks of Loop Quantum Cosmology (LQC) [11,12] and Brane Cosmology (BC) [13–15], respectively, is rather complicated, especially for LQC [16,17]. As a consequence, the new formalism of Deformed Commutation Relations (DCRs) has been developed as a way to easily implement quantum gravitational effects to any Hamiltonian system.

The first and most famous DCR is the Generalized Uncertainty Principle (GUP) representation by Kempf, Mangano and Mann (KMM-GUP), which is inspired by String Theories. By adding a higher-order momentum term in the standard commutator, the corresponding uncertainty relations are modified in such a way that an absolute minimal uncertainty on position appears [18–20]. This is a reminder that it is not possible to probe below the string scale, and the GUP representation is a simple way to introduce the concept of a minimal length expected in QG theories.

The DCRs can then be generalized to other functions of the momentum; different generalizations are possible, but it is these that are usually able to introduce the QG cut-offs of interest [21]. We use three deformations in particular [22]: the Loop Algebra, which introduces a momentum (i.e., energy) cut-off and is able to reproduce effective LQG by replacing singularities with a Bounce; the Brane Algebra, an extended version of the KMM representation, which reproduces Brane Cosmology; and a hybrid between the Loop and the KMM Algebras which we will call the Loop Uncertainty Principle (LUP), which removes singularities through asymptotes. In higher space dimensions, there are some problems, and therefore, for the time being, we will restrict ourselves to the classical limit of these representations, where the DCRs become Deformed Poisson Brackets. However, due to the Jacobi identities, a Non-Commutativity between the position variables will emerge naturally [23,24]. Therefore, these Deformed Algebras represent a straightforward way of introducing QG effects and Non-Commutativity at an effective level in a simple and natural way.

In this paper, however, we are not interested in the removal of cosmological singularities. Rather, we are interested in studying how the chaotic dynamics of the anisotropic Bianchi IX universe [25] is affected by these QG corrections, in a similar vein to what has recently been achieved for the original KMM formulation [26]. We will use Misner variables $(\alpha, \beta_+, \beta_-)$, and it is well known that it is not possible to remove singularities when using the logarithmic variable α instead of scale factors or other powers; indeed, the nature of the resulting modified dynamics seems to strongly depend on what variable is chosen to be modified [27–30].

The Bianchi models are homogeneous but anisotropic cosmological models. There are nine classes, each corresponding to the Lie Algebra of a different three-dimensional group. The interest of studying them lies in their generality, in particular the Bianchi type VIII and Type IX models, which present chaotic dynamics towards the singularity. Indeed, Bianchi IX, also dubbed Mixmaster [25], is the most general homogeneous cosmological model that presents an isotropic limit. In Misner variables, the Mixmaster dynamics are those of a point particle in the (β_+, β_-) plane, constrained in an exponentially steep potential well with the symmetry of an equilateral triangle; the particle universe will keep reflecting off these potential walls indefinitely towards the singularity, and the dynamics acquire a chaotic character. Besides being the starting point for the general inhomogeneous cosmological solution [31,32], its chaotic dynamics make it the perfect arena to test and study quantum corrections and quantum gravitational effects. Indeed, there are many different studies of the Bianchi IX model (and of its inhomogeneous extension) with different approaches; for some examples related to LQC, see [28,33–38].

Therefore, here, we will consider the Mixmaster model in terms of Misner variables. After performing a reduction that allows us to use the isotropic variable α as time [39], we will deform the anisotropy variables $\beta_\pm$, which together form a 2D space that will therefore present Non-Commutativity between the two variables β_+ and β_-. As a consequence, the reflection law against the potential walls will be modified, and the chaotic dynamics will change. In particular, we find that the sign of the quantum gravitational correction in the Deformed Poisson Brackets will determine the type of change. When there is a plus sign, the trajectory will oscillate between two almost-constant angles, similarly to [26]; on the other hand, when there is a minus sign, the number of reflections is finite and the particle universe slows down, until no reflections happen anymore and the singularity is reached with Kasner-like free-particle dynamics [40]. Furthermore, similar initial conditions will yield similar dynamics. Therefore, in all cases, we can claim that QG corrections are able to remove chaos. This study represents an advancement towards the characterization of QG effects in a more general cosmological setting.

The manuscript is organized as follows. In Section 2, we present the classical Bianchi IX model, with particular focus on its chaotic dynamics. In Section 3, we introduce the framework and main properties of the Deformed Commutation Relations. They will then be used in Section 4 to study the fate of chaos and to derive the modified Belinskii–Khalatnikov–Lifshitz maps that classically describe the chaotic dynamics. We then conclude the manuscript with a summary and discussion in Section 5. We will use natural units $\hbar = c = 8\pi G = 1$.

2. The Bianchi IX Model

In this section, we present the most important results about the Bianchi IX dynamics towards the cosmological singularity, i.e., the Mixmaster model [25,41]. It is the most generic homogeneous but anisotropic model and its relevance lies in the possibility of using this description to construct the generic cosmological solution [31,32].

The line element in the Misner variables is

$$ds^2 = -N(t)^2 dt^2 + \frac{1}{4}e^{2\alpha}(e^{2\beta})_{ij}\sigma_i\sigma_j, \tag{1}$$

where $N(t)$ is the Lapse function parametrizing the freedom of choosing different time variables, σ_i has three differential forms depending on the Euler angles of the $SO(3)$ group of symmetry, and β_{ij} is a diagonal, traceless matrix that can be parametrized in terms of the two independent variables (β_+, β_-) as $\beta_{ij} = \text{diag}(\beta_+ + \sqrt{3}\beta_-, \beta_+ - \sqrt{3}\beta_-, -2\beta_+)$. The Misner variables $(\alpha, \beta_\pm)$ represent a very convenient choice to parametrize the Bianchi IX line element, since the information on the evolution of the universe volume $v = e^{3\alpha}$ is separated from the anisotropic content of the model, parametrized by the variables (β_+, β_-). Moreover, in the Misner variables, the Hamiltonian of the model is diagonal in its kinetic part, as one can see from the below formula:

$$\mathcal{H} = \frac{N}{3(8\pi)^2}e^{-3\alpha}\left(-p_\alpha^2 + p_+^2 + p_-^2 + 3(4\pi)^4 e^{4\alpha}V(\beta_\pm)\right) = 0, \tag{2}$$

where $(p_\alpha, p_\pm)$ are the conjugate momenta to $(\alpha, \beta_\pm)$, respectively. Due to spatial curvature[1], there is also a potential term $V(\beta_\pm)$ depending only on the anisotropy variables, whose explicit form is

$$V(\beta_\pm) = 2e^{4\beta_+}\left(\cosh\left(4\sqrt{3}\beta_-\right) - 1\right) - 4e^{2\beta_+}\cosh\left(2\sqrt{3}\beta_-\right) + e^{-8\beta_+}. \tag{3}$$

This term defines a closed potential well with exponentially steep walls and the symmetry of an equilateral curvilinear triangle with open corners at infinity, as we can see in Figure 1. In addition, potential walls move outward while approaching the cosmological singularity $(\alpha \to -\infty)$, due to the term $e^{4\alpha}$ in (2).

The most interesting properties of the Bianchi IX dynamics emerge when applying the Arnowitt–Deser–Misner (ADM) reduction [39]. In particular, if we choose α as an internal time and hence solve the Hamiltonian constraint with respect to the variable p_α, the Mixmaster dynamics becomes isomorphic to that of a two-dimensional point particle, i.e., a point universe, that moves inside a potential well in which the spatial directions are identified by the two anisotropy variables (β_+, β_-). The reduced ADM Hamiltonian is

$$\mathcal{H}_{\text{ADM}} := -p_\alpha = \sqrt{p_+^2 + p_-^2 + 3(4\pi)^4 e^{4\alpha}V(\beta_\pm)} \tag{4}$$

and the classical dynamics of the model can be studied by solving the corresponding Hamilton equations[2]

$$\begin{cases} \dot{\beta}_\pm = \dfrac{p_\pm}{\mathcal{H}_{\text{ADM}}}\,, \\[2mm] \dot{p}_\pm = -\dfrac{e^{4\alpha}}{2\mathcal{H}_{\text{ADM}}}3(4\pi)^4\dfrac{\partial V(\beta_\pm)}{\partial \beta_\pm}\,, \\[2mm] \dot{\mathcal{H}}_{\text{ADM}} = \dfrac{6(4\pi)^4 e^{4\alpha}V(\beta_\pm)}{\mathcal{H}_{\text{ADM}}}\,. \end{cases} \tag{5}$$
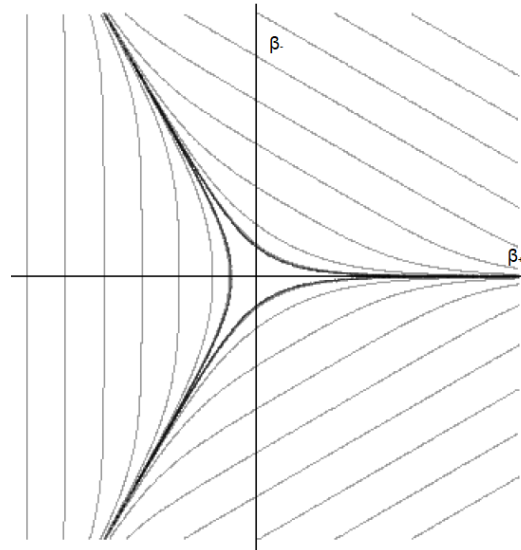

Figure 1. Equipotential lines of the Bianchi IX potential in the (β_+, β_-) plane. Credits: [28].

Because of the steepness of the walls, the point universe acts as a free particle for most of the motion, except when it is reflected off one of the three walls. In particular, using the free-particle approximation[3], i.e., reducing to the Bianchi I model

$$\mathcal{H}^I = \sqrt{p_+^2 + p_-^2}\,, \tag{6}$$

(in which $V(\beta_\pm) = 0$), we can derive the velocity of the point universe from Hamilton equations, i.e., the anisotropy velocity

$$\dot{\beta} \equiv \sqrt{\dot{\beta}_+^2 + \dot{\beta}_-^2} = 1\,. \tag{7}$$

Moreover, studying the region in which the potential term is relevant gives information about the position of the walls and their velocity $|\dot{\beta}_{\text{wall}}| = \frac{1}{2}$. Furthermore, combining integrals of motion, it can be demonstrated that every reflection occurs according to the law

$$\frac{1}{2}\sin\left(\theta_i + \theta_f\right) = \sin\theta_i - \sin\theta_f\,, \tag{8}$$

where θ_i and θ_f are the incidence and reflection angles computed with respect to the potential wall's normal. This reflection law is equivalent to the so-called Belinskii–Khalatnikov–Lifshitz (BKL) map for the Kasner indices that appears when using directional scale factors instead of Misner variables [32,40]. Here, we will use the acronym BKL to refer interchangeably to both the reflection law and the BKL map.

By imposing the condition $|\dot{\beta}_\perp| > \dot{\beta}_{\text{wall}}$, one finds that the maximum incidence angle is

$$\theta_{max} \equiv \arccos\left(\frac{1}{2}\right) = \frac{\pi}{3}\,. \tag{9}$$

This result, together with the fact that the system has the symmetry of an equilateral triangle, proves that a reflection against one of the three walls is always possible. In particular, the number of reflections is infinite while the point universe goes towards the initial singularity. Hence, in this picture, the only effect of the potential walls is to randomly change the direction of the free-particle motion between two subsequent reflections, thus generating chaotic dynamics (see Figure 2).
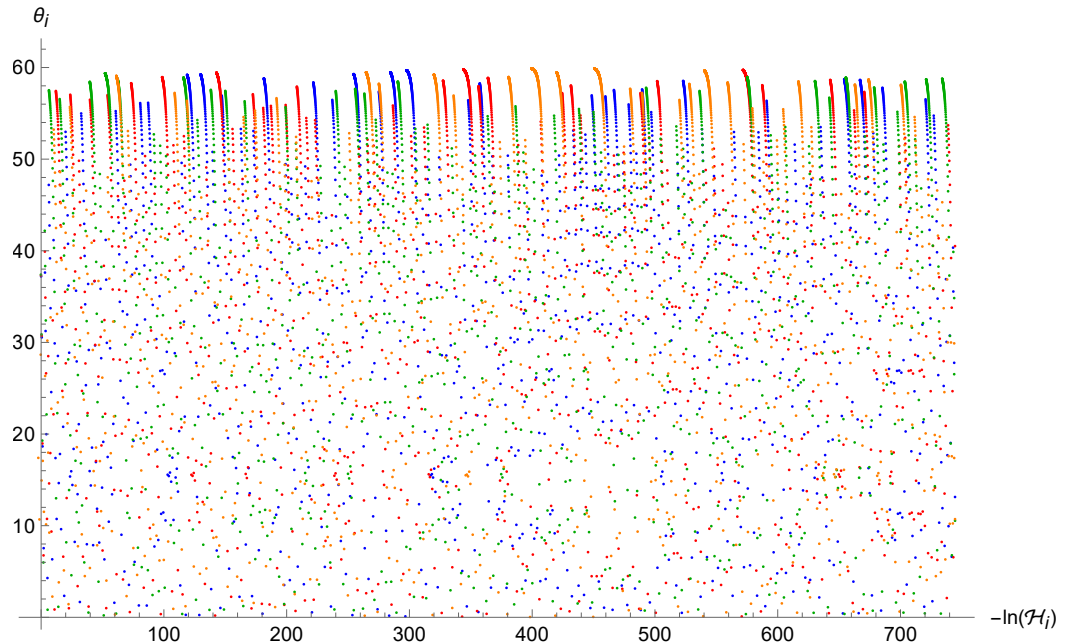
Figure 2. Trajectories of the point universe in the $(\mathcal{H}_i, \theta_i)$ phase space for four different sets of initial conditions in the standard case. It is evident how the point universe explores the entire available phase space showing an ergodic and hence chaotic behavior.

3. Deformed Commutation Relations

In this section, we present the Deformed Commutation Relations that will be later used to deform the anisotropy variables of the Bianchi IX model. The first and most widespread one is the GUP representation in its original KMM formulation, after the authors Kempf–Mangano–Mann [18]. It was developed to easily implement the concept of a minimal length, largely supposed and expected in QG theories. It consists of a deformation of the standard Heisenberg Commutation Relations, which implies a correction to the corresponding uncertainty principle:

$$[\hat{q}, \hat{p}] = i\left(1 + \mu^2 \hat{p}^2\right), \tag{10}$$

$$2\Delta q \Delta p = 1 + \mu^2 \Delta p^2 + \mu^2 \langle \hat{p} \rangle^2. \tag{11}$$

This is the same uncertainty relation that appears in perturbative STs [9,10]. When considering $\langle \hat{p} \rangle = 0$, this implies an absolute minimal uncertainty on position $\Delta q_0 = \mu$. This is interpreted as a reminder that it is not possible to probe lengths smaller than the string length. However, as will also be the case for other forms, once the deformation is implemented, the parameter μ loses any connection to the parent theory and will just play the role of a deformation parameter; this has been explained better in [22] in the cosmological context. Indeed, the parameter μ controls when the corrections are relevant, in that for $\mu \to 0$ (or equivalently for $\langle \hat{p} \rangle \ll 1/\mu$), we recover the standard features. Since the KMM Algebra has already been explored in depth in [26], we will focus on other forms.

We generalize the KMM formulation to other functions of the momentum:

$$[\hat{q}, \hat{p}] = i\,f(\hat{p}). \tag{12}$$

Of course, as mentioned above, it is possible to use even more exotic forms, but we will restrict ourselves to these as they usually give the kinds of cut-off expected from QG theories [21].

First of all, it is important to highlight that these kinds of DCRs are better analyzed in the momentum polarization, meaning that wavefunctions will depend on the momentum as $\psi = \psi(p)$. Then, there are two main operatorial representations: one inspired by the original KMM formulation where the position operator is modified, and one where instead the momentum operator is modified:

$$(1)\quad \hat{q}\,\psi(p) = i\,f(p)\,\frac{\mathrm{d}\psi}{\mathrm{d}p}, \qquad \hat{p}\,\psi(p) = p\,\psi(p), \tag{13a}$$

$$(2)\quad \hat{q}\,\psi(p) = i\,\frac{\mathrm{d}\psi}{\mathrm{d}p}, \qquad \hat{p}\,\psi(p) = g(p)\,\psi(p), \tag{13b}$$

where the function g is related to f through $g^{-1} = \int dp/f(p)$. The equivalence between the two representations is still unclear. They seem to yield compatible results in cosmology when applied to one-dimensional (sub)systems [22]; however, the equivalence seems to fail in higher spatial dimensions, since the second representation is not well defined unless some space–time symmetries are broken [23,24,42].

Regarding higher spatial dimensions, it is natural to generalize the DCRs as

$$\left[\hat{q}_i, \hat{p}_j\right] = i\,\delta_{ij}\,f(\hat{p}_{\text{tot}}), \qquad p_{\text{tot}}^2 = \sum_i p_i^2. \tag{14}$$

In this way, most space–time symmetries are maintained, whereas if the function f depended only on the component along that direction, the symmetries would have been broken. This has some interesting consequences. First, as mentioned earlier, it is impossible to define the function g as in (13b) in a consistent way, and therefore, only the first representation (13a) is available (the position operators $\hat{q}_i$ become derivatives with respect to the corresponding component p_i). Second, in higher space dimensions, the Jacobi identities must be satisfied, and they naturally implement a Non-Commutativity between different space directions [23,24] (the components of the momentum will still commute with each other); in 3D, the commutator can be written as

$$\left[\hat{q}_i, \hat{q}_j\right] = i\,A(\hat{p}_{\text{tot}})\,\hat{J}_{ij}, \tag{15}$$

where the function A depends on f, and J is a deformed angular momentum:

$$A(p) = \frac{f(p)}{p}\,\frac{\mathrm{d}f}{\mathrm{d}p}, \qquad J_{ij} = \frac{q_i\,p_j - q_j\,p_i}{f(p_{\text{tot}})}. \tag{16}$$

This clearly changes the dynamics and gives a possible quantum motivation for Non-Commutative effects. The commutative case is recovered when $f = 1$ and $A = 0$.

In our study, we will be dealing mainly with the classical limit of these DCRs, so we need not worry about operatorial representations at this stage. Indeed, one of the most powerful features of these modified algebras is their straightforward classical limit: the DCRs just become Deformed Poisson Brackets, reading as

$$\{q_i, p_j\} = \delta_{ij}\,f(p_{\text{tot}}), \qquad \{q_i, q_j\} = A(p_{\text{tot}})\,J_{ij}. \tag{17}$$

This makes QG effects easily implementable on any kind of Hamiltonian system, and the effective equations of motion obtain some correction factors:

$$\dot{q}_i = \{q_i, \mathcal{H}\} = \frac{\partial \mathcal{H}}{\partial p_i} f(p_{\text{tot}}) + \sum_{j \neq i} \frac{\partial \mathcal{H}}{\partial q_j} A(p_{\text{tot}}) J_{ij}, \qquad \dot{p} = \{p, \mathcal{H}\} = -\frac{\partial \mathcal{H}}{\partial q} f(p). \tag{18}$$

Let us now present the three specific forms of DCR that we will use in our study[4].

The first one is an extension of the KMM GUP; it is called Brane Algebra because it reproduces the same modified Friedmann equation of Brane Cosmology [22,43]. It takes the form

$$f_{\text{Brane}}(p) = \sqrt{1 + \mu^2 p^2} \,. \tag{19}$$

Except for a factor of 2, the previous KMM function is basically the two leading terms of a Taylor expansion of this one, which is why it is considered an extension. However, interestingly enough, this algebra does not imply an absolute minimal uncertainty on position. The issue is that the square root is a non-local function: when computing the uncertainty relations, we need to perform a Taylor expansion, make the operator act in series form, and then re-sum, but the resummation has a finite convergence radius that does not allow for the same conclusions as the KMM case. The minimal uncertainty is then recovered by imposing an artificial momentum cut-off by hand [44].

The second form is called Loop Algebra because it is inspired by LQC. It takes the form

$$f_{\text{Loop}}(p) = \sqrt{1 - \mu^2 p^2} \,. \tag{20}$$

In one space dimension, the corresponding momentum operator in the representation (13b) would be

$$\hat{p}\, \psi(p) = \frac{\sin(\mu\, p)}{\mu}\, \psi(p), \tag{21}$$

which is the same operator as LQC [11,12]. Indeed, it is able to reproduce exactly the same dynamics as effective LQC: it clearly introduces a momentum cut-off as $\langle \hat{p}^2 \rangle \leq 1/\mu^2$ (otherwise, the commutator would not be purely imaginary anymore and unitarity would be lost). When implemented on the volume (i.e., the cubed scale factor) and its conjugate momentum, which is directly related to energy density and the Hubble parameter through the Hamiltonian constraint, it is able to introduce a cut-off and replace cosmological singularities with a Bounce [22].

The third and final form is called the Loop Uncertainty Principle (LUP), and can be seen as either the counterpart of KMM with a minus sign (indeed, sometimes in the literature, the two are considered together [43]), or as the leading terms of the Taylor-expanded Loop Algebra. It reads as

$$f_{\text{LUP}}(p) = 1 - \mu^2 p^2. \tag{22}$$

In the cosmological context, this algebra has also been able to remove singularities, but instead of a loop-like Bounce, it introduces an asymptotically Einstein-static phase, reproducing what is known as an Emergent Universe [22,45].

In our study, we will implement these three DCRs on the anisotropy variables $\beta_\pm$, which will form a (deformed) two-dimensional space and will therefore not commute between each other anymore:

$$\{\beta_\pm, p_\pm\} = \delta_\pm f(p_{\text{tot}}), \qquad p_{\text{tot}}^2 = p_+^2 + p_-^2, \tag{23a}$$

$$\{\beta_+, \beta_-\} = A(p_{\text{tot}}) \frac{\beta_+ p_- - \beta_- p_+}{f(p_{\text{tot}})}. \tag{23b}$$

As in the classical picture, the isotropic variable α will play the role of time, and therefore will be left undeformed.

4. Bianchi Models with Deformed Poisson Algebras

The aim of this section is to analyze how the Mixmaster dynamics, i.e., the picture of the point particle in a triangular box that falls into the initial singularity, are modified when we consider DCRs in the $(\beta_+, \beta_-, p_+, p_-)$ phase space. As already mentioned, the motion of the point universe for $\alpha \to -\infty$ is that of a free particle, except when it is reflected against a wall. Hence, instead of considering the full Bianchi IX potential, it is possible to consider one wall at a time and use the triangular symmetry to rotate the system, in order to iterate the dynamics. This approximation corresponds to considering the Bianchi II model, whose Hamiltonian is

$$\mathcal{H}^{II} = \sqrt{p_+^2 + p_-^2 + 3(4\pi^4)e^{4(\alpha - 2\beta_+)}},\tag{24}$$

in which we choose only one of the three terms of the full potential (3). This picture describes exactly one single reflection against a potential wall.

Now, we want to study the properties of the dynamics in the framework of DCRs

$$\{p_+, p_-\} = 0,\tag{25a}$$

$$\{\beta_+, \beta_-\} = (\beta_+ p_- - \beta_- p_+)\frac{f'(p_{\text{tot}})}{p_{\text{tot}}},\tag{25b}$$

$$\{\beta_\pm, p_\pm\} = \delta_\pm f(p_{\text{tot}}).\tag{25c}$$

Our interest is understanding if chaos survives in this context. Therefore, we have to construct the modified integrals of motion and then find the modified reflection law that governs how the directions of the point universe before and after a reflection are mapped. In particular, from the modified Hamilton equations

$$\begin{cases} \dot{p}_+ = 3(4\pi^4)f(p)\dfrac{e^{4(\alpha - 2\beta_+)}}{\mathcal{H}^{II}}, \\[2mm] \dot{p}_- = 0, \\[2mm] \dot{\beta}_+ = \dfrac{p_+}{\mathcal{H}^{II}}f(p), \\[2mm] \dot{\beta}_- = \dfrac{p_-}{\mathcal{H}^{II}}f(p) + 3(4\pi)^4\dfrac{(\beta_+ p_- - \beta_- p_+)f'(p_{\text{tot}})}{p_{\text{tot}}}\dfrac{e^{4(\alpha - 2\beta_+)}}{\mathcal{H}^{II}}, \\[2mm] \dot{\mathcal{H}}^{II} = \dfrac{6(4\pi)^4 e^{4(\alpha - 2\beta_+)}}{\mathcal{H}^{II}}, \end{cases}\tag{26}$$

it is easy to see that the constants of motion are

$$p_-, \quad \mathcal{H} - \frac{1}{2}\int_{\bar{p}_+}^{p_+}\frac{1}{f(p_{\text{tot}})}dp'_+.\tag{27}$$

In order to find the modified point-universe velocity, we go back to the Bianchi I approximation, in which the Hamilton equations are

$$\begin{cases} \dot{\mathcal{H}}^I = \dot{p}_+ = \dot{p}_- = 0 \\[2mm] \dot{\beta}_\pm = \dfrac{p_\pm}{\mathcal{H}^I}f(p_{\text{tot}}) \end{cases}\tag{28}$$

and from which we obtain $\dot{\beta} = f(p_{\text{tot}})$. Therefore, in principle, it is not granted that the point particle is always faster than the potential walls. In particular, it can be demonstrated that the wall velocity remains unchanged. Indeed, the condition for the wall to be relevant

is $\mathcal{H}^I/e^{4(\alpha-2\beta_-)} \sim 1$ and it involves only the definition of the Hamiltonian, which is unaffected by DCRs. Hence, we find again $\dot{\beta}_{\text{wall}} = \frac{1}{2}$.

Now, we introduce a convenient parametrization to study the maximum incident angle. In particular, we define

$$(p_-)_{i,f} = \mathcal{H}^I_{i,f} \sin\theta_{i,f} \tag{29a}$$

$$(p_+)_i = -\mathcal{H}^I_i \cos\theta_i, \quad (p_+)_f = \mathcal{H}^I_f \cos\theta_f, \tag{29b}$$

from which we also obtain

$$(\dot{\beta}_-)_{i,f} = f(p_{\text{tot}}) \sin\theta_{i,f}, \tag{30a}$$

$$(\dot{\beta}_+)_i = -f(p_{\text{tot}}) \cos\theta_i, \quad (\dot{\beta}_+)_f = f(p_{\text{tot}}) \cos\theta_f. \tag{30b}$$

Therefore, from the condition $(\dot{\beta}_+)_i > \dot{\beta}_{\text{wall}}$, we find

$$\theta_i < \arccos\left(\frac{1}{2f(p_{\text{tot}})}\right), \tag{31}$$

that is compatible with $\theta_{max} = \frac{\pi}{3}$ in the standard case $f(p_{\text{tot}}) = 1$.

At this point, the strategy to investigate the dynamics is as follows. By using the two constants of motion (27), we obtain the deformed reflection law for a generic $f(p_{\text{tot}})$:

$$\begin{cases} \mathcal{H}_i \sin\theta_i = \mathcal{H}_f \sin\theta_f, \\ \mathcal{H}^i - \frac{1}{2}\int_{\bar{p}_+}^{p_+^i} \frac{1}{f(p'_+, p_-)}\, dp'_+ = \mathcal{H}^f - \frac{1}{2}\int_{\bar{p}_+}^{p_+^f} \frac{1}{f(p'_+, p_-)}\, dp'_+, \end{cases} \tag{32}$$

in which we have used the parametrization (29a) in defining $(p_-)^{i,f}$. Once the initial conditions $(\theta_i, \mathcal{H}_i)$ have been fixed, the map gives the final values $(\theta_f, \mathcal{H}_f)$ after the reflection. Then, in order to completely solve the dynamics, the procedure is iterated using the relation between the final angle θ_f and the new initial angle θ'_i

$$\begin{cases} \theta'_i = \frac{\pi}{3} - \theta_f & \text{if} \quad \theta_f \leq \frac{\pi}{3}, \\ \theta'_i = -\frac{\pi}{3} + \theta_f & \text{if} \quad \theta_f > \frac{\pi}{3}, \end{cases} \tag{33}$$

that can be easily found by using the triangular symmetry of the system. Differently from the standard picture (see Section 2), the condition (31) is not automatically matched after each reflection by the iterated initial angle θ'_i, so it is not given that chaos is still present in the deformed picture.

In the next sections, we will proceed separately for the chosen DCRs, as mentioned in Section 3, and finally we will discuss the results.

4.1. Brane Algebra

Here, we implement the Brane Algebra $f_{\text{Brane}}(p)$ as presented in (19), thus obtaining the following modified symplectic structure for the two anisotropic degrees of freedom (β_+, β_-)

$$\{p_+, p_-\} = 0, \tag{34a}$$

$$\{\beta_+, \beta_-\} = \frac{\mu^2(\beta_+ p_- - \beta_- p_+)}{\sqrt{1 + \mu^2(p_+^2 + p_-^2)}}, \tag{34b}$$

$$\{\beta_\pm, p_\pm\} = \delta_\pm \sqrt{1 + \mu^2(p_+^2 + p_-^2)}. \tag{34c}$$

Hence, the Hamilton equations with these modified Poisson brackets in the Bianchi I approximation are

$$
\begin{cases}
\dot{p}_\pm = 0\,, \\
\dot{\beta}_\pm = \dfrac{p_\pm}{\sqrt{p_+^2 + p_-^2}}\sqrt{1 + \mu^2(p_+^2 + p_-^2)}\,,
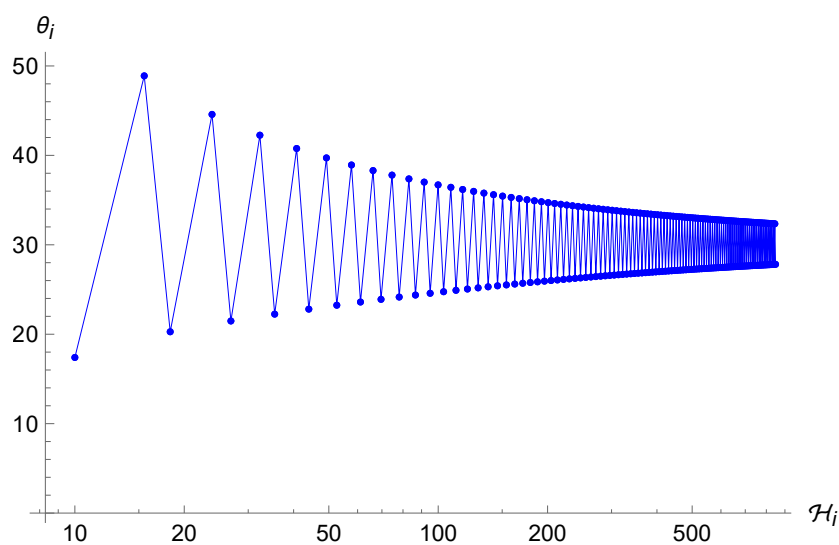\end{cases}
\tag{35}
$$

from which we obtain the modified point-particle velocity, i.e.,

$$
\dot{\beta} = \sqrt{\dot{\beta}_+^2 + \dot{\beta}_-^2} = \sqrt{1 + \mu^2(p_+^2 + p_-^2)} > 1\,.
\tag{36}
$$

As we previously mentioned, the wall velocity is still equal to $\frac{1}{2}$, whereas in this particular algebra, the point particle becomes faster. In principle, this property could suggest the idea that chaos is enhanced in the Brane Algebra framework. To verify this hint, we proceed with the analysis of the BKL map (32), which in this Algebra becomes

$$
\begin{cases}
\mathcal{H}_i \sin\theta_i = \mathcal{H}_f \sin\theta_f\,, \\
\mathcal{H}_i + \dfrac{1}{2\mu}\mathrm{arctanh}\left(\dfrac{\mu\,\mathcal{H}_i \cos\theta_i}{\sqrt{1 + \mu^2\mathcal{H}_i^2}}\right) = \mathcal{H}_f - \dfrac{1}{2\mu}\mathrm{arctanh}\left(\dfrac{\mu\,\mathcal{H}_f \cos\theta_f}{\sqrt{1 + \mu^2\mathcal{H}_f^2}}\right)\,,
\end{cases}
\tag{37}
$$

in which we have used the parametrization (29a) for the definition of $(p_\pm)^{i,f}$. Differently from the standard case (8), this system cannot be solved analytically. Therefore, we need to implement numerical methods to solve the dynamics. In particular, Figures 3 and 4 show the trajectories in the $(\mathcal{H}_i, \theta_i)$ phase space for different initial conditions. As one can see from (31) and (33), the condition for a reflection is always met when $f(p_{\mathrm{tot}}) = f_{\mathrm{Brane}}(p_{\mathrm{tot}})$ and the point particle experiences an infinite series of reflections while falling into the initial singularity. However, the motion loses its chaotic feature and sets into an oscillatory orbit. Indeed, as one can see from Figures 4 and 5, the trajectories tend to become very close to each other for both very similar and sufficiently different initial conditions. In particular, they seem to oscillate ever closer to the value $\pi/6$ which, thanks to the combination of the first equation of (33) and the structure of the map (37) for large values of $\mathcal{H}$, becomes an attractor value.

Figure 3. Trajectory of the point universe in the $(\mathcal{H}_i, \theta_i)$ phase space for the Brane Algebra. The energy $\mathcal{H}_i$ keeps increasing (differently from the standard case where it always decreases), whereas the angle θ_i oscillates indefinitely between two converging values.
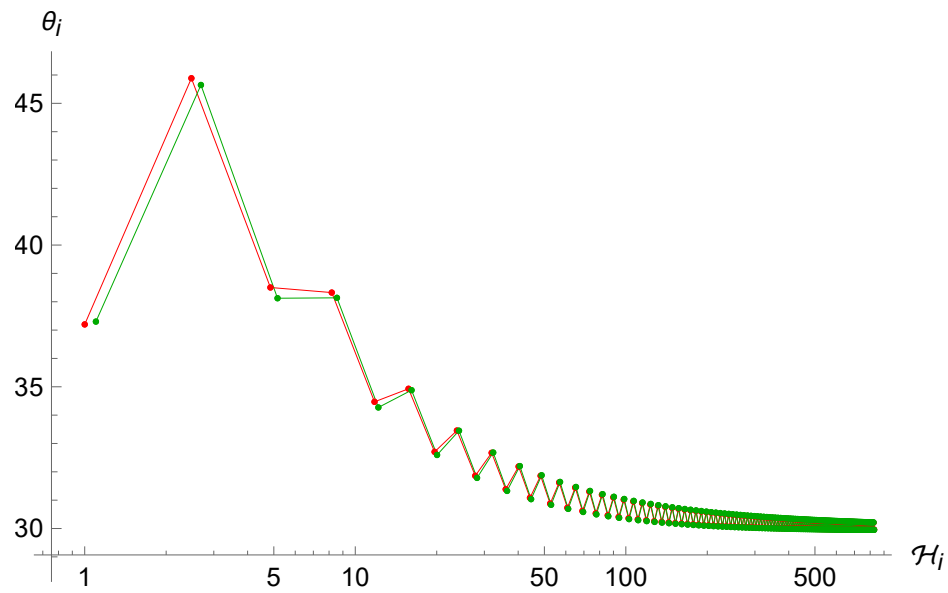
Figure 4. Trajectories of the point universe in the $(\mathcal{H}_i, \theta_i)$ phase space for two different (similar) sets of initial conditions in the Brane Algebra. It is evident that the two trajectories are not sensitive to the initial conditions.
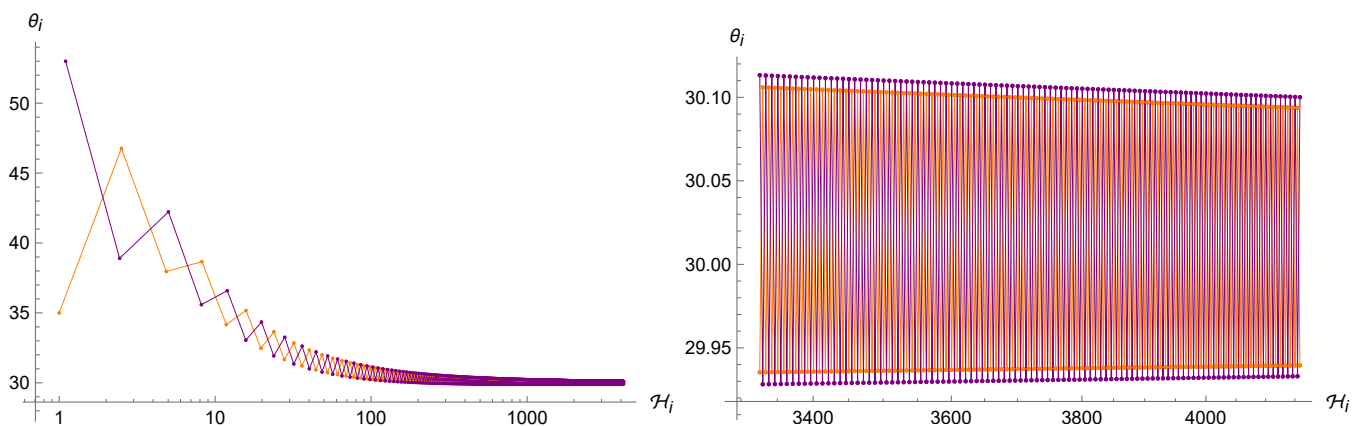
Figure 5. Left: trajectories of the point universe in the $(\mathcal{H}_i, \theta_i)$ phase space for two (sufficiently) different sets of initial conditions in the Brane Algebra. After thousands of iterations, both converge to the same angle of $\pi/6$. Right: same figure, zoomed to the last few hundred iterations.

4.2. Loop Algebra

Now, we study the motion of the point universe in the Algebra inspired by LQC f_{Loop} (see (20)), for which the modified algebra for the anisotropies reads as

$$\{p_+, p_-\} = 0 \,, \tag{38a}$$

$$\{\beta_+, \beta_-\} = -\frac{\mu^2 \left(\beta_+ p_- - \beta_- p_+ \right)}{\sqrt{1 - \mu^2 (p_+^2 + p_-^2)}} \,, \tag{38b}$$

$$\{\beta_\pm, p_\pm\} = \delta_\pm \sqrt{1 - \mu^2 (p_+^2 + p_-^2)} \,, \tag{38c}$$

and the Hamilton equations in the Bianchi I approximation are

$$\begin{cases} \dot{p}_\pm = 0 \,, \\ \dot{\beta}_\pm = \dfrac{p_\pm}{\sqrt{p_+^2 + p_-^2}} \sqrt{1 - \mu^2 (p_+^2 + p_-^2)} \,. \end{cases} \tag{39}$$

While $\dot{\beta}_{\text{wall}}$ remains unchanged, for the point-universe velocity, we find

$$\dot{\beta} = \sqrt{\dot{\beta}_+^2 + \dot{\beta}_-^2} = \sqrt{1 - \mu^2(p_+^2 + p_-^2)} < 1 \tag{40}$$

Hence, the condition (31) is not always met. In particular, when that happens, the iteration map stops, the reflections end, and the point particle keeps moving indefinitely with a free motion towards the initial singularity. For this reason, we expect chaos to be suppressed in this scenario.

As in the previous case, we write down the modified BKL map for the considered Algebra, i.e.,

$$\begin{cases} \mathcal{H}_i \sin\theta_i = \mathcal{H}_f \sin\theta_f\,, \\ \mathcal{H}_i + \dfrac{1}{2\mu}\arctan\left(\dfrac{\mu\,\mathcal{H}_i\cos\theta_i}{\sqrt{1 - \mu^2\mathcal{H}_i^2}}\right) = \mathcal{H}_f - \dfrac{1}{2\mu}\arctan\left(\dfrac{\mu\,\mathcal{H}_f\cos\theta_f}{\sqrt{1 - \mu^2\mathcal{H}_f^2}}\right), \end{cases} \tag{41}$$

and we study the properties of the motion by numerically solving the iterative system, once given initial conditions $(\mathcal{H}_i, \theta_i)$ and checking at every step that condition (31) is satisfied. In the below figures, trajectories for different initial conditions are represented.

In particular, it is even more evident in this case the ergodicity is completely lost with respect to the Brane Algebra scenario (see Figures 6–8). As anticipated above, the system tends again to oscillate between two very close values of θ_i, even with very different choices of initial conditions, before stopping after a finite number of iterations when the term $\mu^2\mathcal{H}^2$ is of order unity, which makes the point-universe velocity very small. Furthermore, we see again that there is an attractor value, this time at $\pi/4$. This is probably due to the fact that in order to observe enough reflections, we must give a very small initial condition for $\mathcal{H}_i$; therefore, we can expand the arctangents around zero and simplify the map (41), which for $\theta_i \approx \pi/4$ yields $\theta_f \approx \pi/12$, and thanks to (33), the next θ_i' will again be around $\pi/4$.
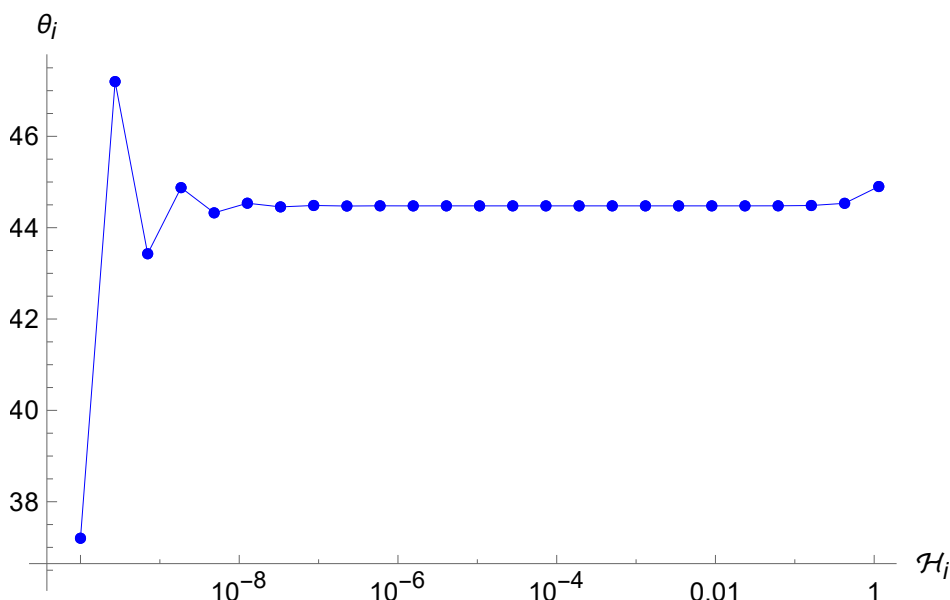
Figure 6. Trajectory of the point universe in the $(\mathcal{H}_i, \theta_i)$ phase space for the Loop Algebra. The energy $\mathcal{H}_i$ keeps decreasing whereas the angle θ_i oscillates between two close values, before stopping after 25 iterations.
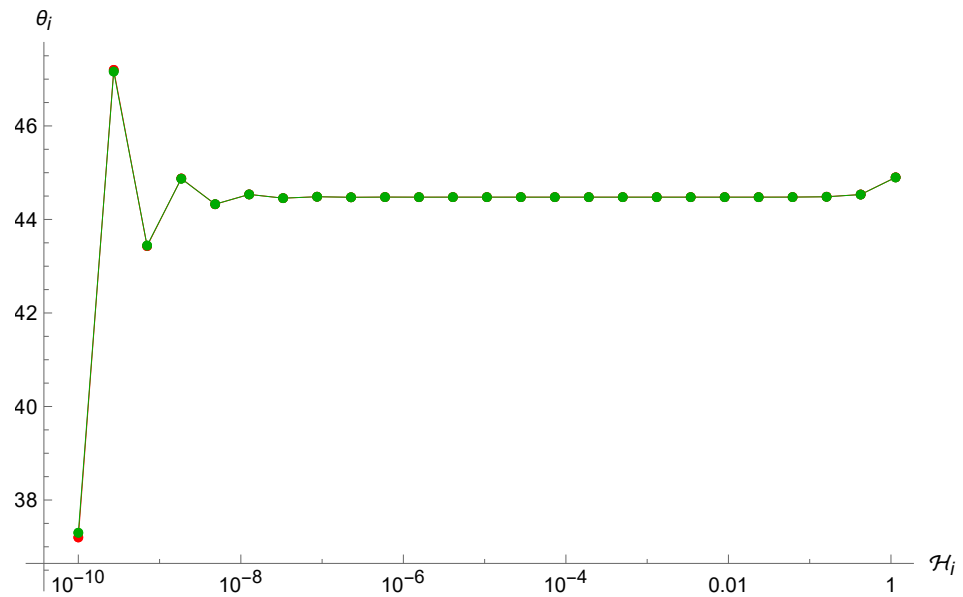
Figure 7. Trajectories of the point universe in the $(\mathcal{H}_i, \theta_i)$ phase space for two different (similar) sets of initial conditions in the Loop Algebra. It is evident that the two trajectories are not sensitive to the initial conditions.
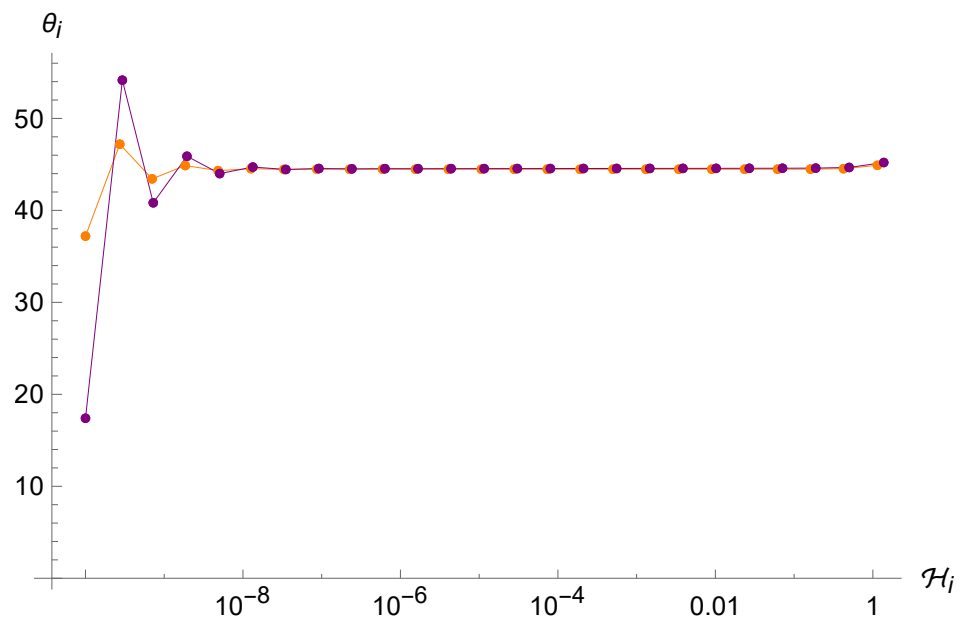
Figure 8. Trajectories of the point universe in the $(\mathcal{H}_i, \theta_i)$ phase space for two different sets of initial conditions in the Loop Algebra. The two trajectories seem to converge even if they started far from each other.

4.3. LUP Algebra

Finally, we analyze the properties of the point-universe dynamics in the LUP Algebra, where f_{LUP} (see (22)) contains only the leading terms of the expansion of f_{Loop}, as discussed in Section 3. In this framework, the modified algebra for the phase space of the anisotropies is

$$\{p_+, p_-\} = 0, \tag{42a}$$

$$\{\beta_+, \beta_-\} = -2\mu^2 \left(\beta_+ p_- - \beta_- p_+\right), \tag{42b}$$

$$\{\beta_\pm, p_\pm\} = \delta_\pm \left(1 - \mu^2(p_+^2 + p_-^2)\right), \tag{42c}$$

and the corresponding Hamilton equations in the Bianchi I approximation are

$$\begin{cases} \dot{p}_\pm = 0\,, \\ \dot{\beta}_\pm = \dfrac{p_\pm}{\sqrt{p_+^2 + p_-^2}} \left(1 - \mu^2(p_+^2 + p_-^2)\right). \end{cases} \tag{43}$$

Similarly to what happens with the Loop Algebra, the point universe is slower, as the following relation shows:

$$\dot{\beta} = \sqrt{\dot{\beta}_+^2 + \dot{\beta}_-^2} = \left(1 - \mu^2(p_+^2 + p_-^2)\right) < 1\,. \tag{44}$$

Hence, with similar motivations to those explained above, we expect the suppression of chaos once the condition (31) is not satisfied anymore by the constants of motion of the point particle. Then, the reflections stop and the point universe proceeds towards the initial singularity with no more reflections on the potential walls.

In order to show the trajectories of the point universe in this scenario, we numerically study the modified BKL map

$$\begin{cases} \mathcal{H}_i \, \sin\theta_i = \mathcal{H}_f \, \sin\theta_f\,, \\ \mathcal{H}_i + \dfrac{\text{arctanh}\left(\dfrac{\mu\,\mathcal{H}_i\cos\theta_i}{\sqrt{1-\mu^2\mathcal{H}_i^2\sin^2\theta_i}}\right)}{2\mu\sqrt{1-\mu^2\mathcal{H}_i^2\sin^2\theta_i}} = \mathcal{H}_f - \dfrac{\text{arctanh}\left(\dfrac{\mu\,\mathcal{H}_f\cos\theta_f}{\sqrt{1-\mu^2\mathcal{H}_i^2\sin^2\theta_i}}\right)}{2\mu\sqrt{1-\mu^2\mathcal{H}_i^2\sin^2\theta_i}}\,. \end{cases} \tag{45}$$
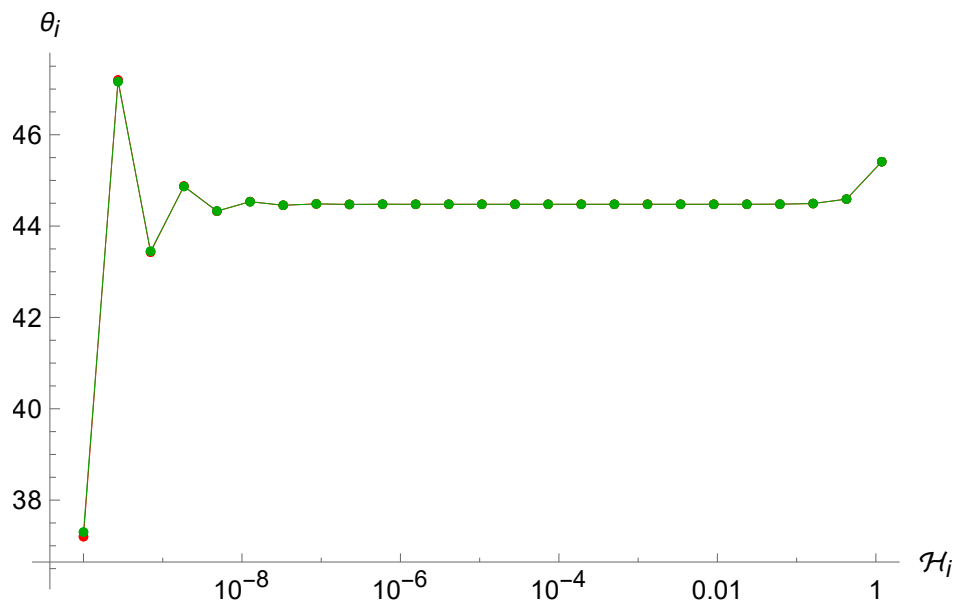
from which we obtain the following trajectories for different sets of initial conditions (Figures 9–11).
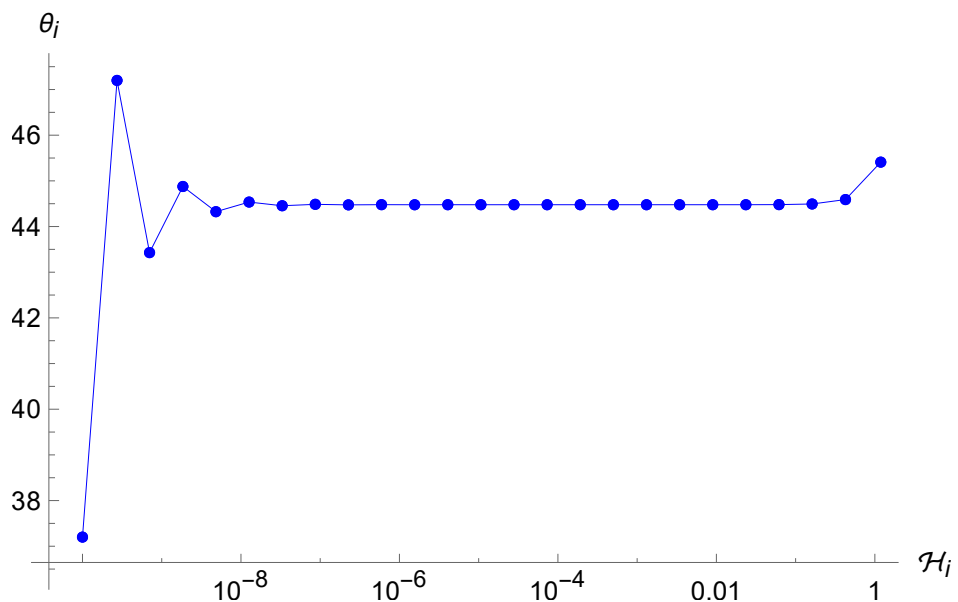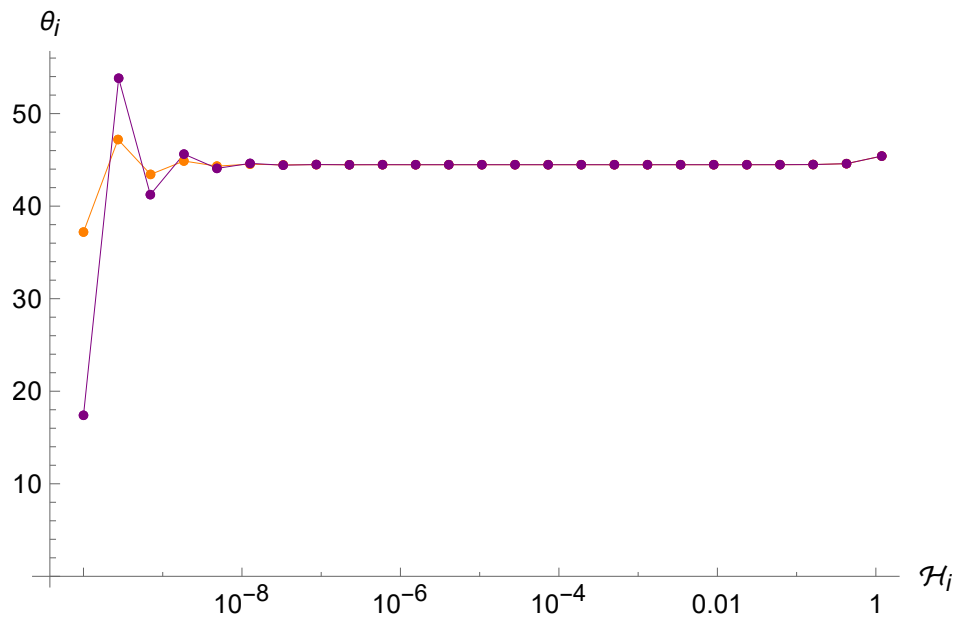

Figure 9. Trajectory of the point universe in the $(\mathcal{H}_i, \theta_i)$ phase space for the LUP Algebra. The energy $\mathcal{H}_i$ keeps decreasing whereas the angle θ_i oscillates between two close values, before stopping after 25 iterations.

Also in this case, the point universe follows oscillatory trajectories before settling into the final uniform rectilinear motion until the singularity is reached. In particular, the ergodic property of the standard motion (see Figure 2) is lost, since trajectories related to similar initial conditions remain close to each other. Analogously to the loop case of Section 4.2, here, we also find an attractor at $\pi/4$. This is to be expected because the

hyperbolic arctangents of the map (45) have the same leading-order behavior for very small arguments of the loop map (41), and therefore, the chain $\theta_i \approx \pi/4$, $\theta_f \approx \pi/12$, $\theta_i' \approx \pi/4$ is also reproduced here.

Figure 10. Trajectories of the point universe in the $(\mathcal{H}_i, \theta_i)$ phase space for two different (similar) sets of initial conditions in the LUP Algebra. It is evident that the two trajectories are not sensitive to the initial conditions.

Figure 11. Trajectories of the point universe in the $(\mathcal{H}_i, \theta_i)$ phase space for two different sets of initial conditions in the LUP Algebra. The two trajectories seem to converge even if they started far from each other.

5. Conclusions

In this study, we analyzed the Bianchi IX model in the Misner variables by implementing DCRs for the two anisotropic variables (β_+, β_-). As shown in [25,31,41], the Bianchi IX universe behaves as a chaotic dynamical system when it approaches the initial singularity, and indeed, the aim of this study was to investigate if chaos survives when a deformed scenario is considered. As demonstrated in [28], when the initial singularity is still present

(as is the case with the isotropic Misner variable, except when pure quantum approaches are considered [46,47]), the only way to affect the chaotic properties of the dynamics is to introduce some kind of cut-off on the real gravitational degrees of freedom, i.e., the anisotropies. Here, we considered three different forms of DCRs inspired by STs and LQC, in order to study how chaos behaves in an effective QG framework. This represents a first step towards the understanding of the quantum properties of the initial singularity, given that the Bianchi IX model can be considered as a building block for the generic cosmological solution [31,32].

In our analysis, we implemented the Brane, Loop and LUP Algebras, as presented in Section 3, on the $(\beta_+, \beta_-, p_+, p_-)$ phase space, obtaining non-trivial Poisson brackets $\{\beta_\pm, p_\pm\}$ and also Non-Commutativity between the configurational variables (β_+, β_-). Obviously, these features resulted in modified Hamilton equations for the Bianchi IX model. In particular, in order to study the dynamics, we first used the Bianchi II approximation by exploiting the triangular symmetry of the system, and then we implemented the Bianchi I approximation since near the initial singularity the potential becomes more and more negligible. With these hypotheses, we found the modified reflection laws in all three cases, i.e., the modified BKL maps which encode the chaotic properties of the dynamics. Differently from the standard case, numerical methods were needed to solve the dynamics, and the interesting result is that chaos does not survive in any of the three scenarios. In particular, in the case of Loop and LUP Algebras, the velocity of the point universe is damped, and therefore, sooner or later it will become slower than the potential walls and there will be no more reflections. This is the effective imprint of the underlying quantum theory, i.e., LQC, in which the deformation parameter μ corresponds to the non-zero step of the lattice implemented on the anisotropies (β_+, β_-), and hence introduces a maximum value for the momenta (p_+, p_-) [12,30].

On the other hand, for the Brane Algebra, the point-universe velocity is greater than in the standard case. However, this is not sufficient to infer the preservation of chaos, and indeed the behavior of the BKL map is similar to that in [26], where the DCR contains only the leading terms of the expansion. The parent theory of these two Algebras, i.e., ST, considers the string scale as the minimal measurable length; when referring to the anisotropies (β_+, β_-), this minimal uncertainty implies that on a quantum level, the corners between the walls are widened and the probability of escaping from the potential well is enhanced [26] (of course, this property must be properly studied in the full quantum regime). From this perspective, it would be interesting to analyze how chaos is modified when the effects of QG theories are introduced directly at the level of the Hamiltonian, without acting on the structure of the Poisson Algebra, similarly to [22].

So far, the relevance of this analysis lies in the possibility of inferring the semiclassical properties of the Mixmaster dynamics in the context of BC and LQC using the Deformed Algebra framework, especially focusing on the fate of chaos. In particular, it seems to be a strong classical property that can be easily suppressed by quantum gravitational effects.

Conflicts of Interest: The authors declare no conflicts of interest.

Notes

[1] The Bianchi IX model reduces to the closed FLRW universe in the isotropic limit.

[2] The dot denotes the derivative with respect to α.

[3] Due to the regression of the walls, the free-particle approximation becomes more and more valid as the particle goes towards the singularity.

[4] Note that in [22], the algebras had slightly different names.

References

1. Hawking, S.W.; Penrose, R. The singularities of gravitationl collapse and cosmology. *Proc. R. Soc. Lond. A* **1970**, *314*, 529. [CrossRef]
2. Hawking, S.W.; Penrose, R. *The Nature of Space and Time*; Princeton University Press: Princeton, NJ, USA, 1996.
3. Rovelli, C.; Smolin, L. Loop space representation of quantum General Relativity. *Nucl. Phys. B* **1990**, *331*, 80. [CrossRef]
4. Rovelli, C.; Smolin, L. Spin networks and quantum gravity. *Phys. Rev. D* **1995**, *52*, 5743. [CrossRef] [PubMed]
5. Ashtekar, A.; Lewandowski, J.; Marolf, D.; Mourão, J.; Thiemann, T. Quantization of diffeomorphism invariant theories of connections with local degrees of freedom. *J. Math. Phys.* **1995**, *36*, 6456. [CrossRef]
6. Ashtekar, A.; Pullin, J. *Loop Quantum Gravity: The First 30 Years*; World Scientific: Singapore, 2017. [CrossRef]
7. Ashtekar, A.; Bianchi, E. A short review of Loop Quantum Gravity. *Rep. Prog. Phys.* **2021**, *84*, 042001. [CrossRef] [PubMed]
8. Green, M.; Schwarz, J.; Witten, E. *Superstring Theory (Cambridge Monographs on Mathematical Physics)*; Cambridge University Press: Cambridge, UK, 1987.
9. Amati, D.; Ciafaloni, M.; Veneziano, G. Can Space-Time Be Probed Below the String Size? *Phys. Lett. B* **1989**, *216*, 41. [CrossRef]
10. Amelino-Camelia, G.; Mavromatos, N.E.; Ellis, J.; Nanopoulos, D.V. On the Space–Time Uncertainty Relations of Liouville Strings and D-Branes. *Mod. Phys. Lett. A* **1997**, *12*, 2029. [CrossRef]
11. Bojowald, M. Loop Quantum Cosmology. *Living Rev. Relativ.* **2005**, *8*, 11. [CrossRef]
12. Ashtekar, A.; Singh, P. Loop Quantum Cosmology: A status report. *Class. Quantum Gravity* **2011**, *28*, 213001. [CrossRef]
13. Maartens, R.; Koyama, K. Brane-World Gravity. *Living Rev. Relativ.* **2010**, *13*, 5. [CrossRef]
14. Brax, P.; van de Bruck, C. Cosmology and brane worlds: A review. *Class. Quantum Gravity* **2003**, *20*, R201. [CrossRef]
15. Langlois, D. Brane Cosmology: An introduction. *Prog. Theor. Phys. Suppl.* **2002**, *148*, 181. [CrossRef]
16. Bojowald, M. Critical Evaluation of Common Claims in Loop Quantum Cosmology. *Universe* **2020**, *6*, 36. [CrossRef]
17. Cianfrani, F.; Montani, G. A critical analysis of the cosmological implementation of Loop Quantum Gravity. *Mod. Phys. Lett. A* **2012**, *27*, 1250032. [CrossRef]
18. Kempf, A.; Mangano, G.; Mann, R.B. Hilbert space representation of the minimal length uncertainty relation. *Phys. Rev. D* **1995**, *52*, 1108. [CrossRef] [PubMed]
19. Maggiore, M. A generalized uncertainty principle in quantum gravity. *Phys. Lett. B* **1993**, *304*, 65. [CrossRef]
20. Scardigli, F. Generalized uncertainty principle in quantum gravity from micro-black hole gedanken experiment. *Phys. Lett. B* **1999**, *452*, 39. [CrossRef]
21. Hossenfelder, S. Minimal Length Scale Scenarios for Quantum Gravity. *Liv. Rev. Rel.* **2013**, *16*, 2. [CrossRef] [PubMed]
22. Barca, G.; Giovannetti, E.; Montani, G. Comparison of the semiclassical and quantum dynamics of the Bianchi I cosmology in the polymer and GUP extended paradigms. *Int. J. Geom. Methods Mod. Phys.* **2022**, *19*, 2250097. [CrossRef]
23. Fadel, M.; Maggiore, M. Revisiting the algebraic structure of the generalized uncertainty principle. *Phys. Rev. D* **2022**, *105*, 106017. [CrossRef]
24. Segreto, S.; Montani, G. N-Dimensional non-commutative GUP quantization and application to the Bianchi I model. *Eur. Phys. J. C* **2024**, *84*, 796. [CrossRef]
25. Misner, C.W. Mixmaster Universe. *Phys. Rev. Lett.* **1969**, *22*, 1071. [CrossRef]
26. Segreto, S.; Montani, G. Mixmaster Universe in a 2D non-commutative GUP framework. *Preprint* **2024**. [CrossRef]
27. Montani, G.; Mantero, C.; Bombacigno, F.; Cianfrani, F.; Barca, G. Semiclassical and quantum analysis of the isotropic Universe in the polymer paradigm. *Phys. Rev. D* **2019**, *99*, 063534. [CrossRef]
28. Giovannetti, E.; Montani, G. Polymer representation of the Bianchi IX cosmology in the Misner variables. *Phys. Rev. D* **2019**, *100*, 104058. [CrossRef]
29. Giovannetti, E.; Barca, G.; Mandini, F.; Montani, G. Polymer Dynamics of Isotropic Universe in Ashtekar and in Volume Variables. *Universe* **2022**, *8*, 302. [CrossRef]
30. Barca, G.; Giovannetti, E.; Montani, G. An Overview on the Nature of the Bounce in LQC and PQM. *Universe* **2021**, *7*, 327. [CrossRef]

31. Belinskii, V.; Khalatnikov, I.; Lifshitz, E. A general solution of the Einstein equations with a time singularity. *Adv. Phys.* **1982**, *31*, 639. [CrossRef]
32. Montani, G.; Battisti, M.V.; Benini, R.; Imponente, G. *Primordial Cosmology*; World Scientific: Singapore, 2009.
33. Crinò, C.; Montani, G.; Pintaudi, G. Semiclassical and quantum behavior of the Mixmaster model in the polymer approach for the isotropic Misner variable. *Eur. Phys. J. C* **2018**, *78*, 886. [CrossRef]
34. Montani, G.; Battisti, M.V.; Benini, R.; Imponente, G. Classical and quantum features of the Mixmaster singularity. *Int. J. Mod. Phys. A* **2008**, *23*, 2353. [CrossRef]
35. Bojowald, M.; Date, G.; Hossain, G.M. The Bianchi IX model in Loop Quantum Cosmology. *Class. Quantum Gravity* **2004**, *21*, 3541. [CrossRef]
36. Wilson-Ewing, E. Loop Quantum Cosmology of Bianchi type IX models. *Phys. Rev. D* **2010**, *82*, 043508. [CrossRef]
37. Benini, R.; Montani, G. Inhomogeneous quantum Mixmaster: From classical towards quantum mechanics. *Class. Quantum Gravity* **2007**, *24*, 387. [CrossRef]
38. Antonini, S.; Montani, G. Singularity-free and non-chaotic inhomogeneous Mixmaster in polymer representation for the volume of the universe. *Phys. Lett. B* **2019**, *790*, 475. [CrossRef]
39. Arnowitt, R.; Deser, S.; Misner, C.W. Canonical variables for General Relativity. *Phys. Rev.* **1959**, *117*, 6. [CrossRef]
40. Kasner, E. Geometrical Theorems on Einstein's Cosmological Equations. *Am. J. Math.* **1921**, *43*, 217. [CrossRef]
41. Misner, C.W. Quantum Cosmology. I. *Phys. Rev.* **1969**, *186*, 1319. [CrossRef]
42. Barca, G.; Gielen, S. Bouncing Bianchi models with Deformed Commutation Relations. 2025, *in preparation*.
43. Battisti, M.V. Cosmological bounce from a deformed Heisenberg algebra. *Phys. Rev. D* **2009**, *79*, 083506. [CrossRef]
44. Segreto, S.; Montani, G. Extended GUP formulation and the role of momentum cut-off. *Eur. Phys. J. C* **2023**, *83*, 385. [CrossRef]
45. Barca, G.; Montani, G.; Melchiorri, A. Emergent universe model from a modified Heisenberg algebra. *Phys. Rev. D* **2023**, *108*, 063505. [CrossRef]
46. Giovannetti, E.; Montani, G. Is Bianchi I a bouncing cosmology in the Wheeler-DeWitt picture? *Phys. Rev. D* **2022**, *106*, 044053. [CrossRef]
47. Giovannetti, E.; Maione, F.; Montani, G. Quantum Big Bounce of the Isotropic Universe Using Relational Time. *Universe* **2023**, *9*, 373. [CrossRef]